RESEARCH PAPER

Blocked-micropores, surface functionalized, bio-compatible and silica-coated iron oxide nanocomposites as advanced MRI contrast agent

Masih Darbandi · Sophie Laurent · Martin Busch · Zi-An Li ·
Ying Yuan · Michael Krüger · Michael Farle · Markus Winterer ·
Luce Vander Elst · Robert N. Muller · Heiko Wende

Abstract Biocompatible magnetic nanoparticles have been found promising in several biomedical applications for tagging, imaging, sensing and separation in recent years. In this article, a systematic study of the design and development of surface-modification schemes for silica-coated iron oxide nanoparticles (IONP) via a one-pot, in situ method at room temperature is presented. Silica-coated IONP were prepared in a water-in-oil microemulsion, and subsequently the surface was modified via addition of organosilane reagents to the microemulsion system. The structure and the morphology of the as synthesized nanoparticles have been investigated by means of transmission electron microscopy (TEM) and measurement of N_2 adsorption–desorption. Electron diffraction and high-resolution transmission electron microscopic (TEM) images of the nanoparticles showed the highly crystalline nature of the IONP structures. Nitrogen adsorption indicates microporous and blocked-microporous structures for the silica-coated and amine functionalized silica-coated IONP, respectively which could prove less cytotoxicity of the functionalized final product. Besides, the colloidal stability of the final product and the presence of the modified functional groups on top of surface layer have been proven by zeta-potential measurements. Owing to the benefit from the inner IONP core and the hydrophilic silica shell, the as-synthesized nanocomposites were exploited as an MRI contrast enhancement agent. Relaxometric results prove that the surface functionalized IONP have also signal enhancement properties. These surface functionalized

M. Darbandi (✉) · Z.-A. Li · M. Farle · H. Wende
Faculty of Physics and Center for Nanointegration
Duisburg-Essen (CeNIDE), University of
Duisburg-Essen, 47048 Duisburg, Germany
e-mail: masih.darbandi@uni-due.de;
masih.darbandi@vanderbilt.edu

Present Address:
M. Darbandi
Department of Physics and Vanderbilt Institute of
Nanoscale Science and Engineering (VINSE), Vanderbilt
University, Nashville, TN 37234-0106, USA

S. Laurent · L. Vander Elst · R. N. Muller
Department of General, Organic and Biomedical
Chemistry NMR and Molecular Imaging Laboratory,
University of Mons, 7000 Mons, Belgium

M. Busch · M. Winterer
Nanoparticle Process Technology, Faculty of Engineering
and Center for Nanointegration Duisburg-Essen
(CeNIDE), University of Duisburg-Essen, 47048
Duisburg, Germany

nanocomposites are not only potential candidates for highly efficient contrast agents for MRI, but could also be used as ultrasensitive biological-magnetic labels, because they are in nanoscale size, having magnetic properties, blocked-microporous and are well dispersible in biological environment.

Introduction

Recent progresses in the iron oxide nanoparticles (IONP) preparation opens a promising field towards the development of a new generation of magnetic cell labelling and separation, targeted drug delivery and hyperthermia treatments by magnetic particles. In particular, IONP can be utilized as magnetic probes with signal-enhancing capability, which can resolve the weakness of current MRI techniques. Large scale applications of IONP ranging from magnetic devices to molecular biology have prompted the development of several widely used methods for the synthesis of these nanoparticles including sonochemical reactions, sol–gel techniques, host template, coprecipitation, microemulsion, microwave plasma, and mechanical alloying (Yang et al. 2005; Wu et al. 2012, 2010; Jana et al. 2004; Li et al. 2012; Peng and Sun 2007; Zeng et al. 2004; Liu et al. 2005; Huang et al. 2005; Sun et al. 2004; Park et al. 2004).

IONP itself may not be very useful in practical applications because they are extremely reactive, and aggregation or nonspecific adsorption with proteins or other substances would spoil the sensitivity under biological conditions. Most importantly they can be toxic when they are directly exposed to the biological systems. Therefore, further development of applications of IONP require means for incorporating them in

Y. Yuan · M. Krüger
Department of Microsystems Engineering and Freiburg Materials Research Centre, University of Freiburg, Freiburg, Germany

R. N. Muller
Center for Microscopy and Molecular Imaging, 6041 Gosselies, Belgium

various matrixes. On the one hand, this would provide protection and compatibility for the IONP with various environments, and on the other hand, this would impart specific properties of the IONP to the carrier matrix.

Owing to its special advantage over other materials, silica has been considered as one of the most ideal layers for protection of the IONP. Silica shell is chemically inert, robust and optically transparent in the visible region. It can be increased in size by seeded growth, such that the separation between neighbouring particles can be tuned, so that the collective behaviour of the particles can be tailored. Additionally, the silica shell is hydrophilic and biocompatible.

The encapsulation of nanoparticles with silica shell has been the subject of extensive research for several years (Shin et al. 2010; Kamaruddin and Stephan 2011; Graf et al. 2003; Wang et al. 2010; Kobayashi et al. 2001; Liz-Marzàn et al. 1996; Yin et al. 2002). Two main synthetic pathways were developed. The first method relied on the well known Stöber process (Stöber et al. 1968), in which silica was formed in situ through the hydrolysis and condensation of a sol–gel precursor in ethanol: water mixtures under alkaline conditions at room temperature. The second is based on the microemulsion method in which the process is performed in conjunction with the hydrolysis of organometallic precursors such as tetraethoxysilane (TEOS), followed by condensation in the water nanodroplets to form a coating on the nanoparticles within reverse micelle structures (Chung et al. 2011; Mokari et al. 2005; Li et al. 1999; Yi et al. 2005; Selvan et al. 2005; Gao et al. 2003).

Since surface functionalization plays an important role in many biological systems, therefore, any potential application of silica encapsulated IONP requires further derivatization of the silica surface. Such functionalized core–shell structures, are a key in designing complicated structures with promising applications in biomolecular therapeutics and biomedicine.

In this study, the synthesis of IONP, silica encapsulation and subsequently the surface functionalization on the micropores silica shell have been performed in situ via a one-pot method. The outer surface of the functionalized silica shell also offers anchoring sites for the immobilization of biomolecular species of interests (e.g., enzymes, DNA oligomers, and antibodies). The phase, shape, size, structure, porosity and colloidal stability of the yielded product

have been characterised using-transmission electron microscope (TEM), nitrogen adsorption/desorption and zeta-potential techniques. Nitrogen adsorption indicates micropores and blocked-micropores structures for the silica-coated and amine functionalized silica-coated IONP, respectively, which could prove less cytotoxicity of the functionalized final product. Finally, in view of their usage as contrast enhancing agent in MRI, the relaxivity of the synthesized nanocomposites has been recorded over a wide range of magnetic field on a Fast Field Cycling Relaxometer.

Experimental section

Chemicals

All of the chemicals were used as received, without further purification. Tetraethyl orthosilicate (TEOS), 3-aminopropyltris(methyloxy)silane (APS), 3-mercaptopropyltris(methyloxy)silane (MPS) were from Sigma–Aldrich company. Ammonia aqueous solution, cyclohexane, acetone, butanol, propanol, and ethanol were from Sigma–Aldrich as analytical grade.

Preparation

Preparation of IONP

In the synthesis process, a microemulsion was first prepared by mixing 800 µl of aqueous solution of iron salt, composed of 0.1 M $FeCl_2$ and 0.2 M $FeCl_3$, and 1.6 ml IGEPAL® CO-520 as surfactant (Polyoxyethylene (5) nonylphenylether) in 15 ml of cyclohexane as a continuous phase in a three-neck flask with vigorous stirring under N_2 atmosphere at room temperature. The resulting suspension was clear to the eye. Five minutes after the microemulsion system was formed, 200 µl aqueous ammonia solution (33 wt%) was introduced to the reactor. The formation of the nanoparticles was visually observed by the appearance of a black color of the mixture.

The nanoparticles were precipitated from the microemulsion using acetone and then centrifugated. The resultant precipitate of particles was washed (for each washing step and subsequent centrifugation, a sonicator bath was used to completely disperse the precipitate into the corresponding solvent and remove any physically adsorbed molecules from the particle

surfaces). The final product was dispersed in pure water (as IONP).

Preparation of silica-coated IONP

For synthesis of silica-coated IONP, first IONP were synthesized as mentioned in "Preparation of IONP" section (without washing process), then 150 µl of TEOS (tetraethyl orthosilicate) as a precursor for silica formation, were added in a flask 5 min after the addition of ammonia aqueous solution to initiate the encapsulation process. Subsequently, the reaction mixture was aged for 24 h at room temperature with vigorous stirring. After the reaction was completed, the nanoparticles (as silica-coated IONP) were precipitated and washed as described in "Preparation of IONP" section.

Preparation of surface functionalized silica-coated IONP

For the preparation of surface functionalized silica-coated IONP, after synthesis of silica-coated IONP which were mentioned in "Preparation of silica-coated IONP" section (without washing), 100 µl diluted organosilane (APS) was added to the same water-in-oil microemulsion, 30 min after the addition of TEOS. Then the reaction mixture was aged for 24 h at room temperature with vigorous stirring. After the reaction was completed, the nanoparticles (as surface functionalized silica-coated IONP) were precipitated and washed as described in "Preparation of IONP" section (Scheme 1).

Characterization

The TEM samples were prepared by casting one drop of suspension containing IONP on the Cu-TEM grid coated with an amorphous carbon thin film and then dried in air. The TEM and energy-dispersive analysis of X-ray emission (EDAX) and selected area electron diffraction (SAED) characterization were carried out in a Phillips CM 12 transmission electron microscope operating at 120 kV and Tecnai F20 operating at 200 kV.

The zeta-potential (or the overall surface charge) of nanoparticle samples in solution was determined using a Nanosizer ZS (Malvern Instruments, Malvern, UK). The temperature of measurement was set to 25 °C.

Scheme 1 From IONP towards surface functionalized, bio-compatible, blocked-micropores and silica-coated nanocomposites
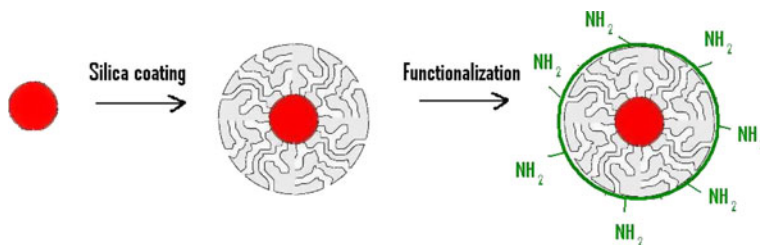
The specific surface area of the samples was investigated in a commercial low temperature nitrogen adsorption analyzer (Quantachrome Autosorb 1C) using the BET method. The pore size distribution was calculated according to the BJH method, thus assuming cylindrical pore geometry.

The Nuclear Magnetic Resonance Dispersion (NMRD) profile was recorded at 37 °C on a Fast Field Cycling Relaxometer (Stelar, Mede, Italy). Particles were dispersed in DMSO, to keep all kind of IONP non-sediment during the measurements. Longitudinal relaxivities were measured over a magnetic field range from 0.24 mT to 0.94 T (0.01–40 MHz). The longitudinal and transversal relaxation times-at 0.47 T and 1.41 T were measured with Minispec Mq-20 and Mq-60 Series systems (Bruker, Karlsruhe, Germany), respectively.

Results and discussions

Representative transmission electron micrograph (TEM) pictures of IONP as well as silica-coated IONP are shown in Fig. 1. The TEM micrographs of IONP and core–shell nanocomposites revealed that they are uniform in size within the useful size range for bio-applications (Eggenberger et al. 2007, 2010). Due to the difference in electron scattering factors between light and heavy elements, the darker contrast indicates the heavy element of Fe or Fe-oxide, while the brighter contrast indicates Silica in the low magnification bright-field micrographs. The element-dependent contrast is further confirmed by high-resolution TEM images, which are shown as insets in Fig. 1. (More TEM results are presented on the supporting material).

The high crystallinity of the IONP core and the amorphous nature of the silica shell are clearly shown in the insets. The size distribution has been determined from the diameter histogram obtained by statistically measuring the size of more than one hundred individual nanoparticles (c, d). The mean diameter of the IONP and silica-coated nanocomposites were 6.3 ± 0.9 and 13.3 ± 1.2 nm respectively. Most importantly, such a small size ranges enhances biological targeting efficiency and specificity.

Figure 2 shows the EDAX analysis of the IONP as well as silica-coated IONP. EDAX analysis confirms the presence of Fe and O in the cores (Fig. 2a) and core–shell nanoparticles (Fig. 2b), and moreover Si in core–shell nanoparticles (the peaks of Cu and C originate from the copper mesh and the carbon film that supported the sample in the TEM analysis). Importantly, no chloride was detected, indicating the absence of un-reacted Fe-precursor. To characterize the crystallinity of the IONP and silica-coated IONP core–shell nanoparticles, we performed Selected Area Electron Diffraction (SAED). Figure 2c shows the SAED pattern consisting of rings which can be indexed with IONP phase (JPCDF: 79-0419, cubic structure, $a = 8.396$ Å) (Haavik et al. 2000; Pecharromán et al. 1995). The sharp rings indicate the high crystallinity of the IONP nanoparticles. Figure 2d depicts the coexistence of a crystalline phase (IONP) and an amorphous phase (SiO_2) in the core–shell particles. It reveals that the silica shell is not crystalline and has amorphous structure, whereas the crystalline phase of IONP are still detectable. (Corresponding XRD pattern of bare and silica-coated IONP are presented in the supporting materials).

Introducing effective functional groups onto the surfaces of silica-coated nanoparticles is interesting because the surface properties of silica-coated nanomaterials could be largely influenced by the nature of the surface functional groups. Especially, the coating of IONP with an amino functional group offers the advantage of further biomodification directly on the surface of the silica-coated nanoparticles, which means its amine group can be exploited for derivatization with biomolecules, drugs and metals. For example (Abou-Hassan et al. 2009) have used a

Fig. 1 TEM/HRTEM micrograph of IONP (**a**) and corresponding diameter distribution histogram (**c**), TEM/HRTEM micrograph of silica-coated IONP (**b**) and corresponding diameter distribution histogram (**d**)
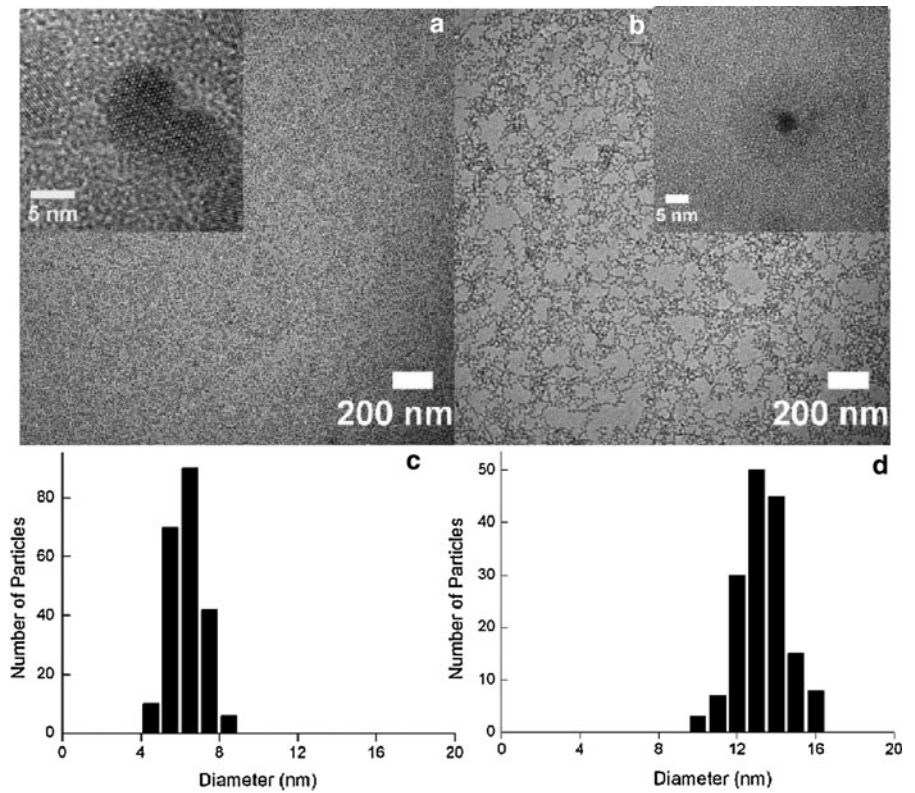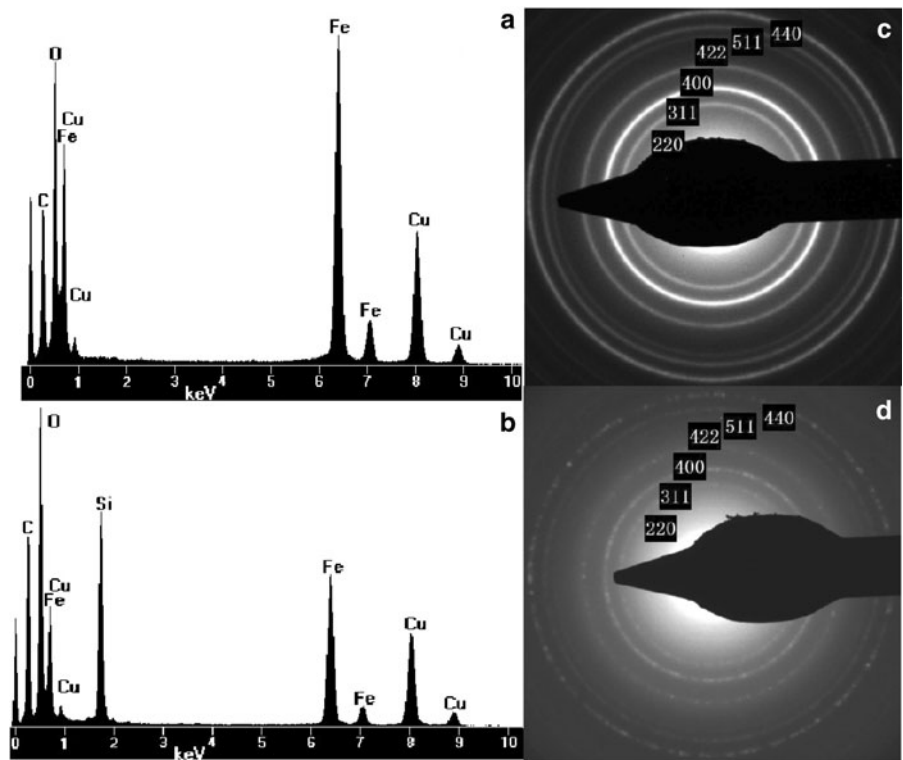

Fig. 2 EDX spectra of IONP (**a**) and corresponding SAED pattern (**c**), EDX spectra of silica-coated IONP (**b**) and corresponding SAED pattern (**d**)

microfluidic platform for multistep synthesis of IONP and silica-coated IONP by using a network of continuous-flow microreactors. In their approach, the multistep continuous coupling of several chemical reactions in different microreactors has been used. In such a system different parameters should be adjusted to get the desired product.

Here we have developed an in situ, one-pot surface functionalization on silica-coated IONP, in which organosilanes (APS) were added to the water-in-oil microemulsion after hydrolyzation reaction of TEOS. The mixtures were then stirred overnight at room temperature.

Nitrogen adsorption and desorption isotherms are used to investigate the specific surface area and porous nature of silica-coated IONP, and surface functionalized IONP (shown in Fig. 3a). The isotherm
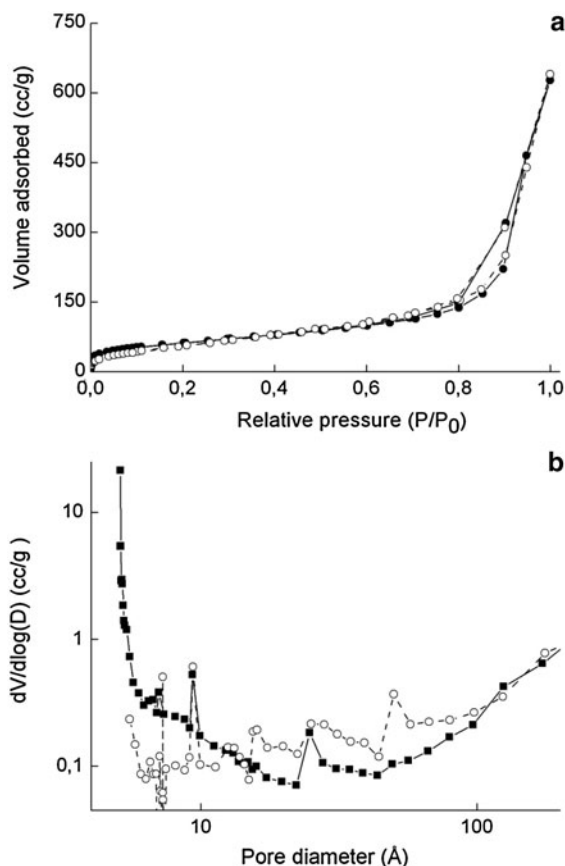

Fig. 3 **a** Nitrogen adsorption–desorption isotherm of: silica-coated IONP (*filled circle*), surface functionalized silica-coated IONP (*open circles*), **b** BJH pore-size distribution of silica-coated IONP (*filled squares*) and surface functionalized silica-coated IONP (*open circles*)

can be categorised as being of type II with a small hysteresis loop. The corresponding Barrett–Joyner–Halenda (BJH) pore size distribution plotted in Fig. 3b, which exhibited a maximum below 0.5 nm (micropores) for silica-coated IONP. But this maximum has been quenched in functionalized silica-coated IONP (blocked-micropores), indicating that pores are blocked by aminosilane surface functionalization compared to non-functionalized IONP. The BET surface area of the silica-coated and functionalized silica-coated IONP were 221 and 217 m^2 g^{-1}, respectively. Therefore, functionalization on silica-coated IONP resulted in a significant loss of micropores, but negligible reduction of the specific surface area. The mechanism of pore generation in silica has been extensively studied by Boissière et al. (2003, 2001).

To prove whether amine groups which block the microporous are directly located at the surface of core–shell nanoparticles or buried within the texture of the silica shell, and also to investigate and compare the respective colloidal stabilities, zeta-potential measurements on the final products were conducted. The zeta-potential is a measurement of the electrical potential (surface charge) close to the particle surface. A high value is beneficial for the electrostatic stabilization of colloidal nanoparticles. At physiological pH 7.4, silica groups have negative charges but the amine groups are positively charged. This can be explained by considering the pKa values of amine and silanol groups on the surface of the nanoparticles, which are 9.0, and 7.0, respectively. Therefore, the amine groups cause positive charges (+31 mV) and the silanol groups negative charges (−36 mV) (cf. Eqs. (1), (2)).

$$R - SiO - H \Leftrightarrow R - SiO^- + H^+ \qquad (1)$$

$$R - NH_2 + H^+ \Leftrightarrow R - NH_3^+ \qquad (2)$$
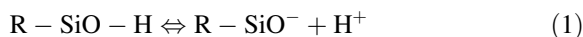
From this measurement it can be concluded, that the addition of APS after TEOS hydrolysis causes the grafting of the amine groups onto the silica surface of the nanoparticles with a high density leading to a blocking of the micropores and causing a large magnitude of the zeta potential and a reversal of the polarity. Bare IONP exhibit a zeta-potential of about −6 mV, and are unstable and aggregate.

Silica-coated IONP and surface functionalized silica-coated IONP were dispersed in pure water and left for one week at room temperature (Fig. 4).

Fig. 4 Silica-coated IONP (*left*), surface functionalized silica-coated IONP (*right*) after 1 week dispersion in pure water

Surprisingly, a biological aggregate was observed in Silica-coated IONP but not at surface functionalized silica-coated IONP (since this experiment was carried out at normal lab conditions, i.e. not sterilized condition, microbial component like bacteria and viruses will be present during the experiment time). The amorphous nature of the silica shell and micropores in the shell wall provides sufficient open channels to enable the inorganic components (most likely iron ions) of the core to be released from the spheres. The released elements could act as nutrient material for biological components and help to grow the biological aggregates. In case of surface functionalized silica-coated IONP the micropores are blocked by functionalization and prevent any biological aggregate growth.

If one could combine the advantages of blocked-microporous silica and magnetic particles to fabricate a nanocomposite with less cytotoxicity and magnetic separability, a novel adsorbent material and targeted drug delivery matrix which carries the drug directly to a specific organ or location in the body under an external magnetic field could be available.

Owing to the benefit from the inner IONP core and the hydrophilic functionalized silica shell, the as synthesized nanocomposites were exploited as an MRI contrast enhancement agent, and their contrast effect
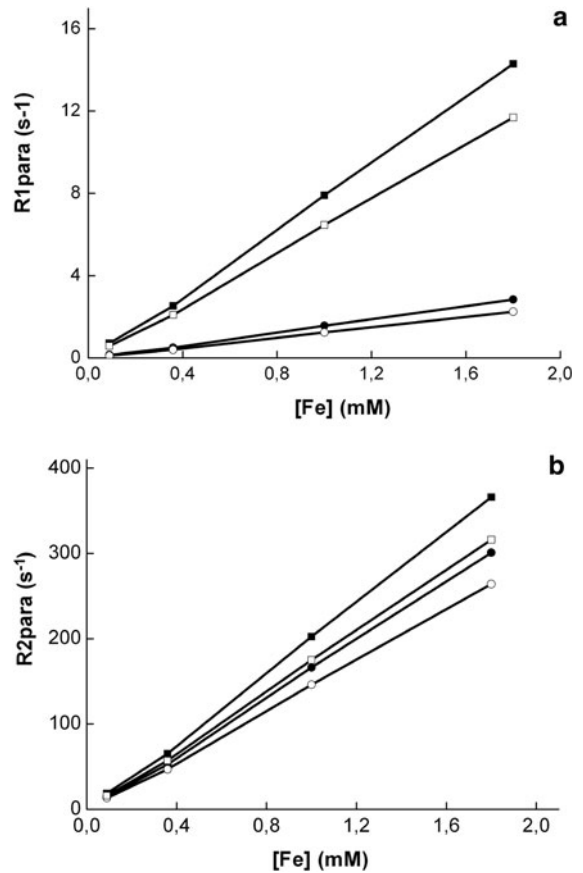

Fig. 5 Relaxivity measurements of IONP: **a** longitudinal relaxation rates at 20 MHz and 60 MHz, **b** transversal relaxation rates at 20 MHz and 60 MHz (in both *graphs lines* are: surface functionalized silica-coated IONP at 20 MHz, silica-coated IONP at 20 MHz, surface functionalized silica-coated IONP at 60 MHz, silica-coated IONP at 60 MHz from up to down respectively)

in solution was tested by using a relaxometric instrument. The relaxation rates R_1 ($1/T_1$) and R_2 ($1/T_2$) were obtained as a function of the iron millimolar concentration for the nanoparticles at 0.47 and 1.41 T. Figure 5a and b show the result of relaxometric measurements (longitudinal and transversal relaxation rates of versus iron concentration). As it can be seen from these figures, R_1 and R_2 relaxation rates vary linearly with iron concentration, according to the Eqs. (3) and (4), respectively:

$$R_1 = \frac{1}{T_1^{\text{obs}}} = r_1[\text{Fe}] + \frac{1}{T_1^{\text{dia}}} \tag{3}$$

$$R_2 = \frac{1}{T_2^{\text{obs}}} = r_2[\text{Fe}] + \frac{1}{T_2^{\text{dia}}} \tag{4}$$

Table 1 Relaxivity values of the IONP at 0.47 and 1.41 T (at 37 °C)

Sample	r_1 at 20 MHz (s^{-1} mM^{-1})	r_2 at 20 MHz (s^{-1} mM^{-1})	r_1 at 60 MHz (s^{-1} mM^{-1})	r_2 at 60 MHz (s^{-1} mM^{-1})
IONP-SiO$_2$	7.9 (0.08)	166.3 (0.1)	1.6 (0.06)	202.5 (0.08)
IONP-SiO$_2$–NH$_2$	6.5 (0.02)	146.1 (0.1)	1.2 (0.03)	174.9 (0.06)
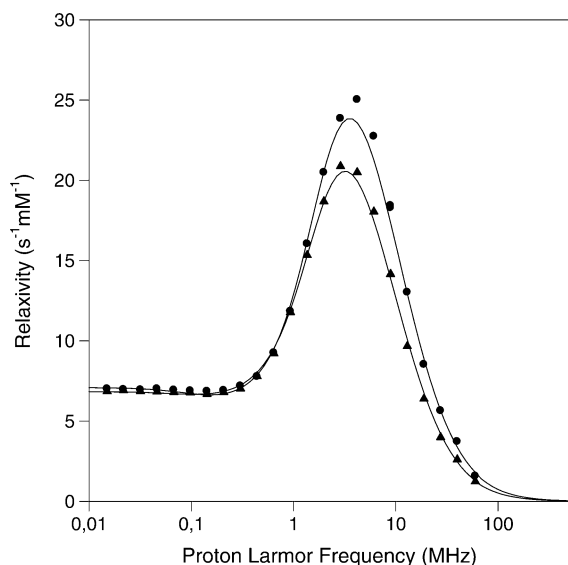
Fig. 6 NMRD profiles of silica-coated IONP (*triangle*) and functionalized silica-coated IONP (*circle*)

Table 2 Values obtained by the NMRD fitting

	Radius (nm)	M_{sat} (A m^2 kg^{-1} of particle)
IONP-SiO$_2$	7.8	22.3 ± 0.4
IONP-SiO$_2$–NH$_2$	8.2	19.5 ± 0.4

where r_1 and r_2 are the longitudinal and transversal relaxivities, respectively. T_1^{dia} and T_2^{dia} are the proton relaxation times in solutions without nanoparticles. The relaxivity is defined as the increase of relaxation rate of solvent protons in 1 mmol L^{-1} solution of contrast agents and its value is expressed in s^{-1} mmol^{-1} L^{-1} in iron. By measuring the relaxation rate of a sample at different iron concentration, relaxivities can be calculated from the slope of relaxation rate versus iron concentrations (Fig. 5).

r_1 and r_2 relaxivities, and r_2/r_1 ratio at different magnetic fields are summarized in Table 1. It is well known that the relaxivity ratio, r_2/r_1, is an important parameter to estimate the efficiency of T$_2$-contrast agents. Our relaxometric result shows that IONP without and with surface functionalization have approximately the same efficiency (silica-coated IONP have little higher values) which means that the surface functionalized IONP could also enhance the MRI signal.

Nuclear magnetic resonance dispersion (NMRD) profiles of nanoparticles are shown in Fig. 6. Interpretation of the relaxation profiles (evaluation of the relaxivity as a function of the magnetic field) with appropriate theoretical models (Roch et al. 1999a, b) provides information about the main properties of the superparamagnetic crystals, such as their specific saturation magnetization and 'waterproof' diameter (Pinho et al. 2012). NMRD profiles have been performed at 310 K (Table 2).

The value of the diffusion coefficient, has been measured by NMR diffusion and was 1.01×10^{-9} m^2 s^{-1}. The magnetization as well as the diameter agrees with the other data. The surface functionalization of IONP causes a decrease of the apparent specific saturation magnetization M_{sat} obtained by relaxometry and an increase of water proof diameter.

Conclusions

A water-in-oil microemulsion based one-pot, in situ surface modification method has been used to successfully prepare uniform silica-coated IONP of the desired surface functionality at room temperature. Base catalysed silica encapsulation was initiated by the addition of tetraethyl orthosilicate (TEOS) to a microemulsion. Subsequently, we performed the functionalization of the latter with an amine terminated surface silane coupling agent (aminopropyl-trimethoxysilane, APS). The resulting terminal NH$_2$ groups can act as conjugation points for biological species. Since this method uses a one-pot procedure,

intermediate purification of nanocomposites is not needed, which means this method is very effective, inexpensive and easy to implement.

Transmission electron microscopy (TEM), and high-resolution TEM, nitrogen absorption–desorption (BET) were used to characterize the products. The BET results prove that silica-coated IONP and functionalized IONP have microporous and blocked-microporous structures respectively. BET surface areas are in the same range for both samples. Zeta-potentials measurements indicate that the amine functional group is mostly located at top of the silica shell blocking the microporous and causing colloidal stability. NMRD results as a prerequisite for clinical and biological application indicates good signal enhancement in both samples independent from the surface functionalization.

In addition to the interesting NMRD properties, amino surface-modification of silica-coated IONP can be implemented very easily to utilize standard bifunctional linker chemistry for conjugation with biomolecules. The resulting conjugates could be used as sensitive and reproducible labels for bioanalytical applications.

References

Abou-Hassan A, Bazzi R, Cabuil V (2009) Angew Chem Int Ed 48:7180

Boissière C, Larbot A, Bourgaux C, Prouzet E, Bunton CA (2001) Chem Mater 13:3580

Boissière C, Martines MAU, Tokumoto M, Larbot A, Prouzet E (2003) Chem. Mater. 15:509

Chung SH, Lee DW, Kim MS, Lee KY (2011) J Colloid Interface Sci 355:70

Eggenberger K, Merkulov A, Darbandi M, Nann T, Nick P (2007) Bioconj Chem 18:1879

Eggenberger K, Frey N, Zienicke B, Siebenbrock J, Schunck T, Fischer R, Bräse S, Birtalan E, Nann T, Nick P (2010) Adv Eng Mater 12:B406

Gao X, Yu KMK, Tam KY, Tsang SC (2003) Chem Commun 24:2998

Graf C, Vossen DLJ, Imhof A, Blaaderen AV (2003) Langmuir 19:6693

Haavik C, Stølen S, Fjellvåg H, Hanfland M, Häusermann D (2000) Am Mineral 85:514

Huang Z, Zhang Y, Tang F (2005) Chem Commun 3:342

Jana NR, Chen Y, Peng X (2004) Chem Mater 16:3931

Kamaruddin S, Stephan D (2011) Catal Today 161:53

Kobayashi Y, Correa-Duarte MA, Liz-Marzàn LM (2001) Langmuir 17:6375

Li T, Moon J, Morrone AA, Mecholsky JJ, Talham DR, Adair JH (1999) Langmuir 15:4328

Li Z, Benzhao H, Faai Z (2012) ACS Appl Mater Interfaces 4:192

Liu F, Cao P, Zhang H, Tian J, Xiao C, Shen C, Li J, Gao H (2005) Adv Mater 17:1893

Liz-Marzàn LM, Giersig M, Mulvaney P (1996) Langmuir 12:4329

Mokari T, Sertchook H, Aharoni A, Ebenstein Y, Avnir D, Banin U (2005) Chem Mater 17:258

Park J, An K, Hwang Y, Park JG, Noh HJ, Kim JY, Park JH, Hwang NM, Hyeon T (2004) Nat Mater 3:891

Pecharromán C, González-Carreno T, Iglesias JE (1995) Phys Chem Miner 22:21

Peng S, Sun S (2007) Angew Chem Int Ed 46:4155

Pinho S, Laurent S, Rocha J, Roch A, Delville MH, Carlos L, Vander Elst L, Muller R, Geraldes C (2012) J Phys Chem 116:2285

Roch A, Gillis P, Ouakssim A (1999a) J Magn Magn Mater 201:77

Roch A, Muller RN, Gillis P (1999b) J Chem Phys 110:5403

Selvan ST, Tan TT, Ying JY (2005) Adv Mater 17:1620

Shin K, Kim JJ, Suh KD (2010) J Colloid Interface Sci 350:581

Stöber W, Fink A, Bohn E (1968) J Colloid Interface Sci 26:62

Sun SH, Zeng H, Robinson DBJ (2004) Am Chem Soc 126:273

Wang YJ, Yan Y, Cui JW, Hosta-Rigau L, Heath JK, Nice EC, Caruso F (2010) Adv Mater 22:4293

Wu W, Xiao XH, Zhang SF, Zhou JA, Fan LX, Ren F, Jiang CZ (2010) J Phys Chem C 114:16092

Wu ZX, Li W, Webley PA, Zhao DY (2012) Adv Mater 24:485

Yang T, Shen C, Li Z, Zhang H, Xiao C, Chen S, Xu Z, Shi D, Li J, Gao H (2005) J Phys Chem B 109:23233

Yi DK, Selvan ST, Lee SS, Papaefthymiou GC, Kundaliya D, Ying JY (2005) J Am Chem Soc 127:4990

Yin Y, Lu Y, Sun Y, Xia Y (2002) Nano Lett 2:427

Zeng H, Li J, Wang ZL, Liu JP, Sun S (2004) Nano Lett 4:4187